



Self assembled flower like CdS–ZnO nanocomposite and its photocatalytic activity



T.K. Jana, A. Pal, K. Chatterjee*

Department of Physics and Technophysics, Vidyasagar University, Midnapore 721102, India

ARTICLE INFO

Article history:

Received 18 July 2013

Received in revised form 26 August 2013

Accepted 27 August 2013

Available online 6 September 2013

Keywords:

CdS–ZnO nanocomposite

Optical behavior

Photocatalysis

ABSTRACT

Self assembled flower like CdS–ZnO nanocomposite has been synthesized by a facile chemical route and the prepared materials have been investigated as catalyst in the photodegradation of rhodamine B (RhB) in aqueous solution facilitated by the effective charge transfer mechanism in this coupled semiconductor system. CdS has been grown first and then petal-like ZnO has been produced to assemble into a flower like nanostructure. XRD, SEM, TEM, EDX have been employed to study the structural, morphological and compositional details of this unique nanostructure. It is observed that a strong quenching of band-edge emission of CdS following the growth of ZnO petal on it which is evidence for the occurrence of charge transfer between CdS and ZnO. The strong photocatalytic activity of this novel nanostructure on RhB has been investigated in details.

© 2013 Elsevier B.V. All rights reserved.

1. Introduction

Inorganic nanostructures are becoming ideal systems for revealing novel phenomena at nanoscale leading towards wide range of applications [1–7]. Depending upon the dimensionality and the capability to tailor the morphology they are becoming essential for smart and functional materials. Variety of geometrical morphology [1,4,8–12] are being investigated for the different nanostructures to explore novel properties out of those materials. Specially the coupled semiconductor nanocomposite, having the synergistic effects among the components, with different geometry [2,3,13–17] are attracting much attention due to the added advantages such as improvement of charge separation, increase in the life time of charge carrier and enhancement of the charge transfer efficiency. The coupled semiconductors or the heterojunction interface of semiconductors matching band potentials are particularly attracting huge attention for their successful implementation in photocatalytic degradation of organic pollutants [13,18–20]. Photocatalytic processes in coupled semiconductors have started to play an important role in environmental remediation as well as in renewable energy generation [14,18–21]. While the organic pollutants introduced into the water systems [22,23] are of great concern for society, photocatalytic degradation can potentially be used for water decontamination using visible or ultraviolet light as the illuminating source. Therefore it is urgent to develop highly efficient photocatalytic materials for pollutant degradation

without having any harmful residues. It is found that to enhance the efficiency, photogenerated charge carriers should be effectively separated and that can be enhanced in the composite materials according to their different band gap structures [18,19,24]. Charge injection from a narrow or mid band gap semiconductor to a wide band gap semiconductor can effectively enhance the charge separation by decreasing the recombination possibilities [25]. Among the different coupled semiconductor nanostructures, in the pursuance of photocatalytic degradation, ZnO based nanocomposites [18,19,26–28] gained extreme importance for its different advantages such as direct band gap [bulk : 3.37 eV], ease of crystallization, anisotropic growth, nontoxicity, higher excitation binding energy of 60 meV, higher electron mobility [$200 \text{ cm}^2 \text{ V}^{-1} \text{ s}^{-1}$] and simplicity in tailoring the morphology. However, owing to its large band gap energy, its photoresponse is largely restricted to the ultraviolet (UV) region which is only the 4% of the total solar spectrum. Coupled semiconductors provide the opportunity to sensitize a wide band gap semiconductor (ZnO, TiO_2) by low/mid band gap semiconductors (CdS, In_2S_3 , Bi_2O_3) which are visible light active materials. Particularly CdS (bulk band gap 2.42 eV), having high optical absorption coefficient and similar lattice structure as ZnO, is one of the most appropriate sensitizer for ZnO. Recently many groups have attempted to address the efficient development of heterojunctions for CdS–ZnO with different morphology [19,21,29,16,30,31]. The study of CdS/ZnO system for photocatalytic effect not only varies in synthesis technique but also has wide variety of efficiency according to the structure of the composite. Different CdS–ZnO systems, e.g. urchin like CdS@ZnO [21], nanotubes arrays of CdS/ZnO [16], partially or fully covered CdS nanoparticles on ZnO nanorods [29], ZnO/CdS core shell nanorods

* Corresponding author. Tel.: +91 9474816352.

E-mail addresses: kuntal2k@gmail.com, kuntal@mail.vidyasagar.ac.in (K. Chatterjee).

[19], CdS nanoparticles/ZnO nanowires heterostructure [31] have been reported addressing several relevant issues. But several key factors like development of facile preparation method, generation of proper lattice interface to facilitate the charge transfer, enhancement of the total activation site i.e. surface area are still remain a challenge for the scientific community.

Here we propose a novel method to tether CdS to ZnO in such a fashion so that self assembled flower like unique nanostructures of CdS–ZnO has been synthesized and the sample shows high photocatalytic activity employing effective charge transfer between two coupled semiconductors. Simple chemical route is adopted for the growth of these novel nanocomposite and structural, chemical and morphological details of the specimen has been studied. A possible growth mechanism has been demonstrated for the better understanding of the materials. Absorption and emission properties of the nanocomposite have been investigated and finally the visible light photocatalytic activity of flower like CdS–ZnO nanostructure for degradation of RhB is studied in details. RhB is taken as model organic dye as it is the important xanthene dye and dye pollutants from the textile industry.

2. Experimental section

All the chemicals are Merck made of analytical grade and used without further purification.

2.1. Preparation of CdS

For preparation of CdS nanoseed, CdCl₂ and Na₂S were used as the reactants with molar ratio 1:1. These precursors were dissolved in distilled water under stirring (20 min). Then Na₂S solution was added drop wise in CdCl₂ solution keeping the solution under constant stirring. The whole system was maintained in ice-bath. The precipitate was centrifuged and washed with distilled water for several times until the pH becomes normal. The final water solution from where the precipitate was taken was also tested with silver nitrate solution to discard the presence of NaCl in the product. Finally, the obtained powder was dried at 100 °C for 2 h in a vacuum furnace to get CdS nanoparticles which will be used as nanoseed for the next synthesis part.

2.2. Preparation of CdS–ZnO nanocomposite

To produce CdS–ZnO nano composite, 0.03 gm CdS nanoparticles were well dispersed (sonicated for 30 min) in 25 ml distilled water (solution A). Separately zinc nitrate solution (B) taking 1.48 gm Zn(NO₃)₂ in 15 ml DI water and NaOH solution (C) taking 0.4 gm NaOH in 10 ml DI water were also prepared.

Then solution B and solution C was added drop wise in solution A under stirring condition for 30 min for the formation of ZnO crystal on the nucleating sites of CdS nanoseeds. After the reaction is over the resultant precipitate was centrifuged and washed with distilled water for several times until the pH becomes 7 and then dried in a vacuum furnace at 100 °C for 2 h to produce CdS–ZnO nanocomposite.

Structural analysis of all the powdered samples were carried out by Rigaku Mini-Flex X-ray diffractometer using Cu K α radiation ($\lambda = 1.54178 \text{ \AA}$) source. Morphological analysis was done by both JEM 2100 Transmission Electron Microscope at an accelerating voltage of 200 keV and FEI, Inspect F Scanning Electron Microscopy. EDX was carried out in S-4200, Hitachi. Optical absorption spectra of the powdered samples were recorded in a UV–Vis 1700 Shimadzu Spectrophotometer and to get these spectra the powdered samples were dispersed in ethyl alcohol and mounted in the sample chamber while pure ethyl alcohol was taken in the reference beam position. In case of photocatalysis study the organic dye RhB was taken in distilled water and the sample was dispersed in that solution. For the PL the sample was taken in powder form and the measurement was carried out in Perkin Elmer LS55 fluorescence spectrophotometer.

3. Result and discussion

3.1. Structural, chemical and morphological study

Fig. 1 shows the XRD analyzed data for as prepared CdS and CdS–ZnO samples both. It is evident from the peaks of the CdS–ZnO sample that the product is well crystalline having no impurity as there is no unmatched peak. All the peaks of the final product are matched either with CdS or ZnO. Interestingly compare to the

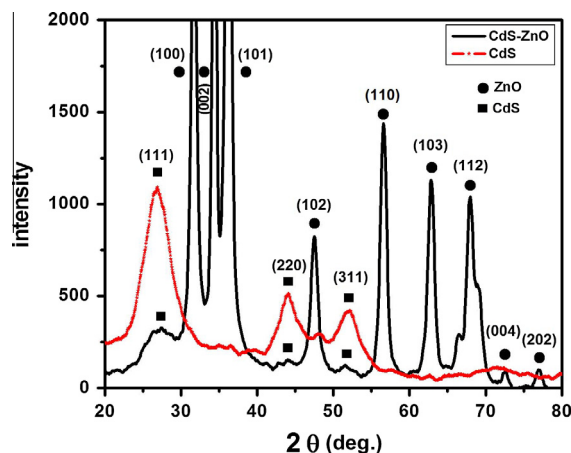


Fig. 1. X-ray diffraction patterns of as prepared CdS and CdS–ZnO nanocomposite.

peak intensity of pure CdS, the peak intensity of CdS–ZnO for CdS phase is noticeably weak. The result is expected [32,33] because the CdS is being shielded for the incoming X-ray by the ZnO in the composite form. It is also very distinct from the peak intensity that ZnO phase is much stronger than the CdS phase in the final product. CdS phase (ICDD card No. 65-2887) has cubic zinc blend structure with lattice constant $a = 5.8320 \text{ \AA}$ where as ZnO phase is matched with ICDD card No. 36-1451 having hexagonal wurtzite crystal structure ($a = b = 3.2495 \text{ \AA}$, $c = 5.2069 \text{ \AA}$).

The photo gallery of Fig. 2 shows the typical SEM and TEM images of the synthesized CdS–ZnO nanocomposite structure. Fig. 2(a)–(c) shows the SEM images at different magnifications and Fig. 2(d)–(f) shows the TEM images at increasing magnification. It is evident from Fig. 2(a) that the synthesized materials has a unique flower like structure where the central part looks much brighter and several petal like protrusion come out at different directions from the center. Fig. 2(b) shows such few CdS–ZnO nanoflowers where it seems the flower has grown partially. In Fig. 2(c) one fully grown flower like structure has been shown. Here the number of petals is higher than the number of petals in the flower like structure shown in Fig. 2(b) and the figure represents the typical structure of a complete CdS–ZnO unit, evolves in this synthesis mechanism. The TEM image shown in Fig. 2(d) also supports the morphology of a flower like structure of the grown composite materials. Here also the central part is much darker and it signifies that the central part is the densest region in these three dimensionally grown structures. Fig. 2(e) shows the magnified version of a petal in the flower structure where it is seen that the petal is formed due to the congregation of several rod like structures. In Fig. 2(f) high resolution TEM shows clearly the aggregation of rods in a part of a petal. The atomic planes visible in the rod shows the unidirectional growth of ZnO and it is evident that the rods are actually made of ZnO to form the petal part of this unique structure. The average total size of a typical CdS–ZnO flower is around 400 nm and the average size of the petal is 100–150 nm. But the rod inside the petal has an average size of 10 nm. The average size of the central core is 90 nm.

As the lattice fringe pattern is not visible in the relatively thick center part of the structure the SAED pattern was taken from that region and the result, shown in Fig. 3(a), matches with the crystal planes of CdS. So, it can be said that the central part of the structure is formed from the seed materials i.e. CdS and the petal parts are made of ZnO which was grown on the latter half of the synthesis procedure. To corroborate the chemical analysis, EDX of the sample was also carried out and the result shows the existence of Cd, S, Zn and O elements. Here the strong Si line was originated from the Si

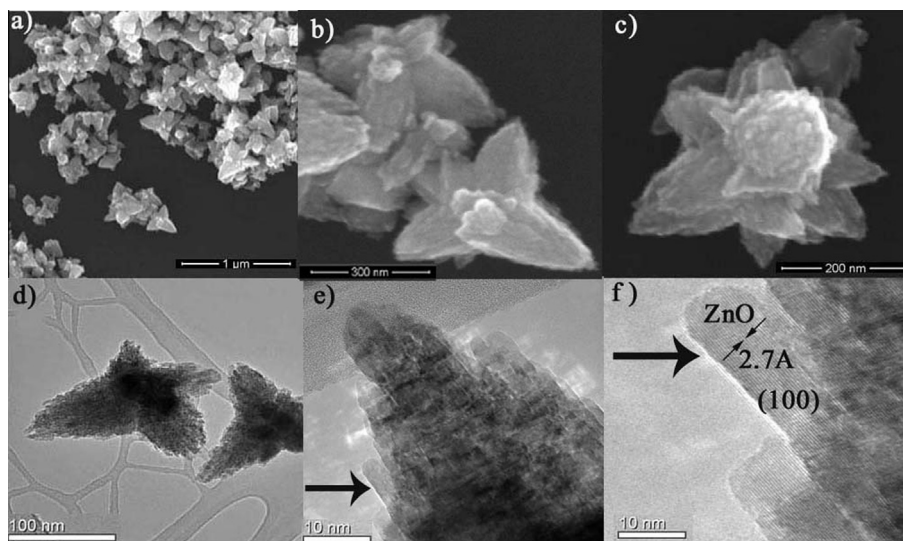


Fig. 2. Typical FESEM (a) – (c), TEM (d) and (e) and HRTEM (f) images of the as prepared CdS–ZnO nanocomposite sample taken at different magnification. The arrow in (e) and (f) indicates the magnification region.

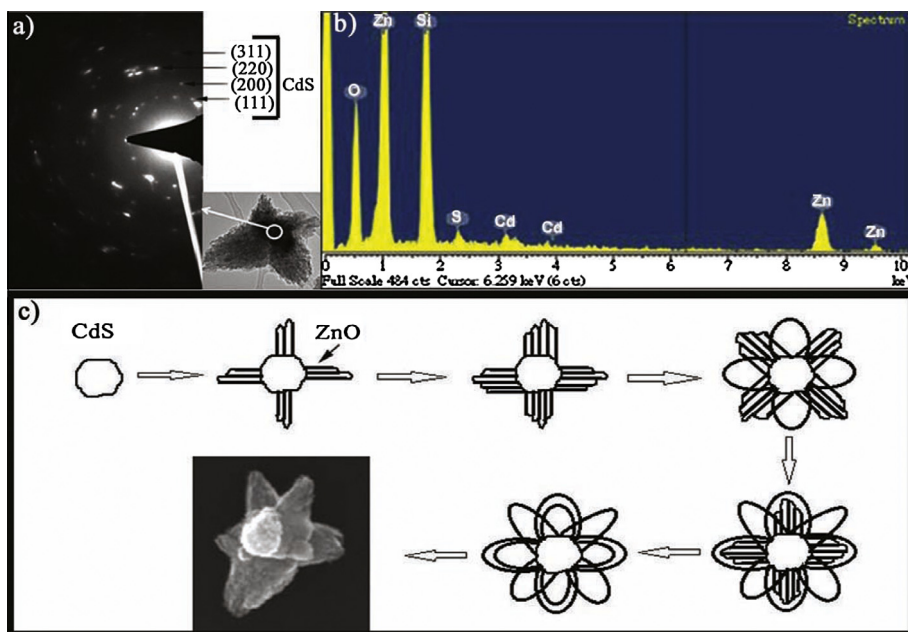


Fig. 3. SAED pattern of the core region (indicated by arrow) of CdS–ZnO nanocomposite with matched crystal planes (a); EDX taken from the as prepared nanocomposite samples deposited on Si wafer (b); and the schematic representation of the growth mechanism of flowerlike CdS–ZnO sample (c).

wafer which was taken as the substrate for the powdered sample to carry out EDX measurement.

3.2. Growth mechanism

Now it is important to understand the evolution of growth process of such unique structure. On the perspective of the results obtained so far, we have proposed a model of growth mechanism which is shown in Fig. 3(c). The model starts with the CdS nanoparticle, grown in the first phase of the synthesis part and such CdS nanoparticles are the nucleating points for the next phase of synthesis. In the next part of synthesis several ZnO nanorods will start to grow initiating from the CdS seeds. The growth of these ZnO nanorods is in the outward directions from the central nucleating site of CdS. As the reaction proceeds the nearby nanorods are self

assembled in such a way that few petal like protrusions form around the central part. This is how the CdS–ZnO nanocomposite starts to take a flower like structure. As the time passes in the reaction several new ZnO nanorods may start to nucleate from the same CdS seed and they eventually grow and assemble just to add new petals in the structure. In the model it is schematically shown that how ZnO nanorods are growing around the seed and how they got assembled to form petals. Eventually the number of such petal increases as the reaction goes on to develop a fully grown flower like CdS–ZnO structure. The last part of the schematic diagram shows SEM image of such typical fully grown CdS–ZnO structure to resemble the model figure. It is to be noticed that Fig. 2(b) and (d) shows some of the typical structure of partially grown nanocomposite. In this case somehow the growth mechanism has been stopped after the formation of first few ZnO

petals. It is found that both fully and partially grown flower like formations are available in the sample morphology. Further investigation is required to reveal the effect and control of different reaction parameters on the evolution of this nanocomposite structure. Though charge transfer characteristic of CdS quantum dot sensitized ZnO flower-like nanostructure have been reported earlier [34] in the category of these coupled semiconductors system but the growth mechanism was not addressed properly. In the category of single semiconductor system, direct observation of growth of MgO nanoflowers by chemical vapor deposition method was also addressed earlier [5]. Here, in our case, the system and structure are different and the development of the structure is given to have the in-depth understanding towards engineering the morphology of such materials.

3.3. Optical characteristics

Fig. 4(a) shows the UV–Vis absorption characteristics of the pure CdS and CdS–ZnO nanocomposite. In the lower panel of Fig. 4(a) the absorption peak for prepared CdS sample is found to be near 470 nm. After formation of the nanocomposite the distinct signature of CdS has been lost and there is no such peak at 470 nm observed in the absorption spectrum shown in the upper panel of Fig. 4(a). The sharp peak in the UV region at around 353 nm is originated from the band edge transition of ZnO. Photoluminescence spectra of CdS and CdS–ZnO nanocomposite samples are shown in Fig. 4(b). It is interesting to note that CdS has strong emission peak near 561 nm along with two other peaks at 530 nm and 544 nm. It is established that surface defects as well as shallow and deep trap states play important role in the luminescence property of CdS. Here the strong emission peak near 561 (2.19 eV) is expected to be linked to the trapped electron/holes at surface defects [35] and peak originated at 530 nm (2.32 eV) corresponds to the defects caused by the interstitial sulfur [36]. But in case of CdS–ZnO nanocomposite the spectrum shows almost quenching of emission peak intensity at 561 nm while the other two peaks in position and intensity are almost remaining same as the pure CdS sample. It signifies that the transfer of electrons from CdS conduction band to ZnO conduction band in the present CdS–ZnO system may inhibit the radiative relaxation of the electrons in CdS energy levels and cause the effective quenching of emission band at 2.19 eV. To make the matter visibly clear the UV-photography of both samples are presented here. Inset near to CdS spectrum in Fig. 4(b) shows yellow luminescence of the CdS sample

dispersed in DI water taken in UV light (254 nm). The photograph for the CdS–ZnO sample taken in same UV source has been shown near to the CdS–ZnO spectrum in Fig. 4(b). Here also it is clear that the luminescence of CdS has been quenched after the formation of CdS–ZnO nanocomposite. These available separated electrons and holes now can effectively be guided towards the activation of other chemical elements and this observation pave the foundation of the possibility that the materials can be utilized in photocatalytic applications.

3.4. Photocatalytic experiments

The photo catalytic activity of CdS–ZnO system was measured by the degradation of RhB in aqueous solution under halogen lamp radiation. In a typical process 10 μM solution of RhB in DI water was taken and the CdS–ZnO sample was added to it to maintain a catalyst concentration of 1 gm L^{-1} . To achieve equilibrium adsorption the organic dye with catalyst solution was stirred in dark for 1 h and after 1 h of stirring no significant change was observed. The solution was then exposed to 1000 W halogen lamp radiation. The beaker was kept in cold water bath to maintain the reaction temperature at 290 K. Actually the radiation from halogen lamp in the NIR region was balanced by keeping the solution always in the room temperature and ensuring that the degradation was only the result of photocatalysis without having any thermal effect. The zero time reading was obtained from the sample solution taken just before turning on the light [37]. Henceforth the sample was taken from the mother solution under the light radiation in regular interval to measure the optical absorbance. Fig. 5(a) shows different absorption spectrum of the sample solution taken at different times. At starting time ($t = 0$) the spectrum presents the normal intense absorption characteristics of RhB at 554 nm. As time passes the photocatalysis reaction goes on and the gradual degradation of the organic dye leads to the subsequent reduction of the absorption peak intensity. The inset in this figure shows the photograph of the dye with catalyst at starting time and after 190 min of light exposure. It is seen that the color of the dye is completely faded away confirming the degradation of the dye molecules. The percentage of degradation measured at different time was calculated by normalizing the peak intensity in term of the starting ($t = 0$) peak intensity of RhB with catalyst. Experiments without radiation of light in presence of catalyst and with radiation of light without the presence of catalyst have also been done. All these data in terms of degradation percentage is presented in

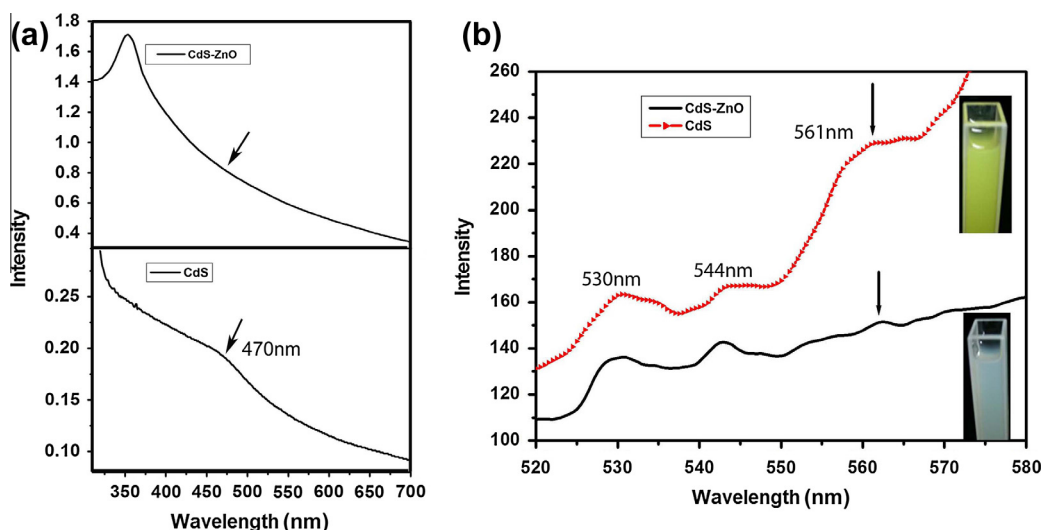


Fig. 4. Optical absorbance spectrum for CdS sample [(a) lower panel] and for CdS–ZnO nanocomposite sample [(a) upper panel]; emission spectra for CdS and CdS–ZnO samples (b). The excitation wavelength is 310 nm for both the case. Inset of (b) panel shows the photograph of respective sample at UV light (254 nm).

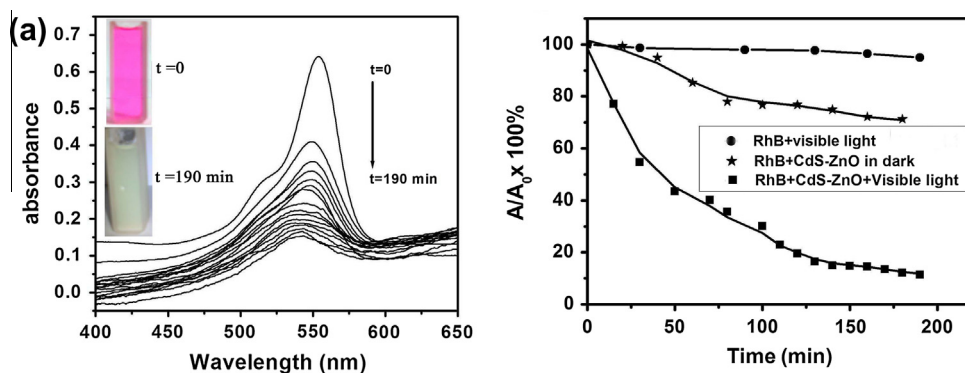


Fig. 5. Absorption spectra of rhodamine B aqueous solution in presence of CdS–ZnO during illumination (a); Decrease in normalized absorption intensity of rhodamine B with respect to time for different cases. Inset in (a) panel shows the photograph of RhB in presence of CdS–ZnO at starting and ending time of illumination.

Fig. 5(b). It is seen that as expected there is no change in degradation of RhB when it is exposed to light without catalyst. In case of RhB with CdS–ZnO catalyst without light radiation there is little change and the dye degraded up to 24% within the measurement duration of 190 min. It seems the catalytic effect of the prepared compound semiconductor is responsible for the slight degradation of this organic dye. But the noteworthy thing is that when the dye with sample is exposed in light the degradation rate is extremely fast and dye is almost completely (90%) decomposed within 190 min. Here it is clear that CdS–ZnO works as strong photo-catalytic agent decolorizing RhB taken as model organic pollutant. The degradation rate constant was calculated from the slope obtained by linear regression from a plot of the natural logarithm of the normalized absorbance as a function of irradiation time [37]. The rate constant is found to be 0.0133/min which is better [38] or comparable [39] to the reported TiO₂ based highly photocatalytic materials. In case of ZnO/CdS system, Ravishankar and his team have shown ZnO/CdS heterostructures with engineered interfaces for high photocatalytic activity and our degradation rate constant is in close match to that of the best sample in the reported series [29]. ZnO/CdS core shell nanorods have also been attempted with variable shell thicknesses to tune the photocatalytic efficiency and it was found that the photodegradation of RhB is better for the higher thickness of CdS shell around ZnO nanorods [19]. Nozaki et al. have demonstrated photocatalytic degradation of 3-4-dihydroxy benzoic acid by CdS–ZnO nanorods, chemically grown on indium tin oxide, but their also it takes comparatively long time (~20 h) to reach the sensible degradation of the dye [40]. ITO/CdS/ZnO composite films were employed for the degradation of methyl orange and the result exhibited that the films prepared under specific conditions have shown higher photocatalytic activity following pseudo first order kinetics of degradation [41]. In our system the structure is unique and the photodegradation capacity is also impressive.

To address the photocatalytic effect in details we propose a possible charge transfer mechanism in our synthesized system and it is shown in Fig. 6(a) as a modified energy band diagram, presented on the canvas of the synthesized materials. The band position of CdS–ZnO system [19,21,34] clearly elucidate the feasibility of charge transfer from CdS to ZnO due to more negative potential of CB and VB edges of CdS than those of ZnO. Furthermore for enhanced photoresponse a faster rate of charge transport is needed and it is facilitated by the intimate and effective contact of the hybrid materials. Here the flower like structure of CdS–ZnO provides the opportunity for better intersystem electron transfer. According to Anderson's model type II heterojunction is formed between CdS and ZnO. Visible light from halogen lamp generates electron–hole pair in CdS and the photogenerated electrons in CdS core can easily move to ZnO petals by the process of ballistic diffusion [40]. Once

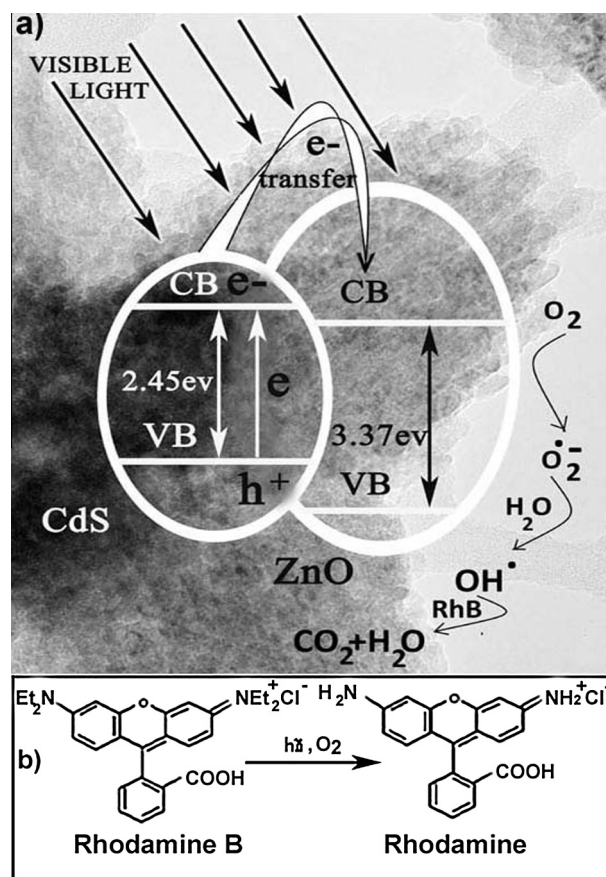


Fig. 6. The schematic photodegradation process in the CdS–ZnO/RhB aqueous solution (a); N-deethylation of rhodamine B to rhodamine (b) [33].

the electrons diffuse into the conduction band of ZnO the recombination probability becomes small as there can be no free hole in ZnO under visible excitation. On the other hand remaining part of the photogenerated excitons i.e. holes are accumulated in the VB of CdS as they cannot move towards more positive VB of ZnO. Now the holes in VB of CdS can react with water adhering to the surface to convert the OH into highly reactive OH[•] and electrons in CB of ZnO can potentially convert the dissolved oxygen into highly oxidative radicals O₂^{•-} which in turn produces OH[•] [39,42]. This O₂^{•-} can react with a H⁺ of solvent water to form OOH[•] and this OOH[•] can eventually generate H₂O₂ and finally OH[•]. The strong OH[•] radicals decompose the organic dye. It is also reported [43] that

OOH[•] and OH[•] are necessary to N-deethylation of RhB which is the basic requirement for the complete degradation of the dye. Fig. 6(b) shows the N-deethylation of RhB to Rh [44]. In this way photogenerated electrons and holes in the synthesized CdS–ZnO nanoflower system effectively degrade the organic dye and present the system as a potential material for future study.

4. Conclusion

In conclusion we have demonstrated simple route to prepare unique flower like CdS–ZnO nanostructure. The evolution of complete self assembled growth mechanism has been proposed on the basis of the results obtained from different chemical and structural investigations. The excellent coupling of the two semiconductors enhanced the charge separation capability and was supported by the photoluminescence study. The novel structure manifests strong photocatalytic activity and is explained on the basis of effective charge separation and charge transfer mechanism in the prepared system. The synthesis method is general and applicable to a wide range of coupled system for photocatalytic and for other possible photo conversion applications.

Acknowledgments

This work was financially supported by the DST-FASTTRACK, India [SR/FTP/PS/11/2009] and Special Assistance Program-UGC, India. A. Pal also thankfully acknowledges his fellowship from UGC–BRS Scheme, India. The authors sincerely thank Prof. Jason Chang, IOP, Academia Sinica, Taiwan for his thoughtful discussions and for providing SEM/EDX facilities.

References

- [1] L. Hu, J. Yan, M. Liao, H. Xiang, X. Gong, L. Zhang, X. Fang, An optimized ultraviolet–A light photodetector with wide range photoresponse based on ZnS/ZnO biaxial nanobelt, *Adv. Mater.* 24 (2012) 2305–2309.
- [2] S.K. Panda, S. Chakrabarti, B. Satpati, P.V. Satyam, S. Chaudhuri, Optical and microstructural characterization of CdS–ZnO nanocomposite thin films prepared by sol–gel technique, *J. Phys. D: Appl. Phys.* 37 (2004) 628–633.
- [3] A.M. Schultz, P.A. Salvador, G.S. Rohrer, Enhanced photochemical activity of α -Fe₂O₃ films supported on SrTiO₃ substrates under visible light illumination, *Chem. Commun.* 48 (2012) 2012–2014.
- [4] X. Fang, L. Wu, L. Hu, ZnS nanostructure arrays: a developing material star, *Adv. Mater.* 23 (2011) 585–598.
- [5] X.-S. Fang, C.-H. Ye, L.-D. Zhang, J.-X. Zhang, J.-W. Zhao, P. Yan, Direct observation of the growth process of MgO nanoflowers by a simple chemical route, *Small* 1 (4) (2005) 422–428.
- [6] X. Fang, J. Yan, L. Hu, H. Liu, P.S. Lee, Thin SnO₂ nanowires with uniform diameter as excellent field emitters: a stability of more than 2400 minutes, *Adv. Funct. Mater.* 22 (2012) 1613–1622.
- [7] H. Liu, L. Hu, K. Watanabe, X. Hu, B. Dierre, B. Kim, T. Sekiguchi, X. Fang, Cathodoluminescence modulation of ZnS nanostructures by morphology, doping and temperature, *Adv. Funct. Mater.* 23 (2013) 3701–3709.
- [8] C.Y. Jiang, X.W. Sun, G.Q. Lo, D.L. Kwong, Improved dye-sensitized solar cells with a ZnO-nanoflower photoanode, *Appl. Phys. Lett.* 90 (2007) 263501–263503.
- [9] Z.R. Dai, Z.W. Pan, Z.L. Wang, Novel nanostructures of functional oxides synthesized by thermal evaporation, *Adv. Funct. Mater.* 13 (2003) 9–24.
- [10] X. Fang, Y. Bando, U.K. Gautam, C. Ye, D. Golberg, Inorganic semiconductor nanostructures and their field-emission applications, *J. Mater. Chem.* 18 (2008) 509–522.
- [11] Z.W. Pan, Z.R. Dai, Z.L. Wang, Growth and structure evolution of novel tin oxide diskettes, *J. Am. Chem. Soc.* 124 (2002) 8673–8680.
- [12] Z.W. Pan, Z.R. Dai, Z.L. Wang, Nanobelts of semiconducting oxides, *Science* 291 (2001) 1947–1949.
- [13] S. Khanchandani, S. Kundu, A. Patra, A.K. Ganguli, Band gap tuning of ZnO/In₂S₃ core/shell nanorod arrays for enhanced visible-light-driven photocatalysis, *J. Phys. Chem. C* 117 (2013) 5558–5567.
- [14] P. Sudhagar, S. Chandramohan, R.S. Kumar, R. Sathyamoorthy, C.H. Hong, Y.S. Kang, Fabrication and charge-transfer characteristics of CdS QDs sensitized vertically grown flower-like ZnO solar cells with CdSe cosensitizers, *Phys. Stat. Sol. A* 208 (2011) 474–479.
- [15] N. Ghows, M.H. Entezari, Sono-synthesis of core–shell nanocrystal (CdS/TiO₂) without surfactant, *Ultrason. Sonochem.* 19 (2012) 1070–1078.
- [16] X. Qi, G. She, Y. Liu, L. Mu, W. Shi, Electrochemical synthesis of CdS/ZnO nanotube arrays with excellent photoelectrochemical properties, *Chem. Commun.* 48 (2012) 242–244.
- [17] Y. Tak, S.J. Hong, J.S. Lee, K. Yong, Fabrication of ZnO/CdS core/shell nanowire arrays for efficient solar energy conversion, *J. Mater. Chem.* 19 (2009) 5945–5951.
- [18] S. Balachandran, M. Swaminathan, Facile fabrication of heterostructured Bi₂O₃–ZnO photocatalyst and its enhanced photocatalytic activity, *J. Phys. Chem. C* 116 (2012) 26306–26312.
- [19] S. Khanchandani, S. Kundu, A. Patra, A.K. Ganguli, Shell thickness dependent photocatalytic properties of ZnO/CdS core–shell nanorods, *J. Phys. Chem. C* 116 (2012) 23653–23662.
- [20] L. Wang, H. Wei, Y. Fan, X. Liu, J. Zhan, Synthesis, optical properties and photocatalytic activity of one-dimensional CdS@ZnS core–shell nanocomposites, *Nanoscale Res. Lett.* 4 (2009) 558–564.
- [21] D. Barpuzary, Z. Khan, N. Vinothkumar, M. De, M. Qureshi, Hierarchically grown urchinlike CdS@ZnO and CdS@Al₂O₃ heteroarrays for efficient visible-light-driven photocatalytic hydrogen generation, *J. Phys. Chem. C* 116 (2012) 150–156.
- [22] Z.Z. Cohen, C. Eiden, M.N. Lobber, in: W.Y. Gerne (Ed.), ACS Symposium Series, vol. 315, American Chemical Society, Washington, DC, 1986.
- [23] L. Muszkat, D. Raucher, M. Magaritz, D. Ronen, in: U. Zoller (Ed.), Ground Water Contamination and Control, Marcel Dekker Inc., NY, 1994, pp. 257–272.
- [24] D.J. Yang, H.W. Liu, Z.F. Zheng, Y. Yuan, J.C. Zhao, E.R. Waclawik, W.B. Ke, H.Y. Zhu, An efficient photocatalyst structure, TiO₂(B) nanofibers with a shell of anatase nanocrystals, *J. Am. Chem. Soc.* 131 (2009) 17885–17893.
- [25] H. Zhou, Y. Qu, T. Zeida, X. Duan, Towards highly efficient photocatalysts using semiconductor nanoarchitectures, *Energy Environ. Sci.* 5 (2012) 6732–6743.
- [26] Y. Zhang, T. Xie, T. Jiang, X. Wei, S. Pang, X. Wang, D. Wang, Surface photovoltage characterization of a ZnO nanowire array/CdS quantum dot heterogeneous film and its application for photovoltaic devices, *Nanotechnology* 20 (2009) 155707–155713.
- [27] J.B. Baxter, E.S. Aydil, Nanowire-based dyesensitized solar cells, *Appl. Phys. Lett.* 86 (2005) 053114–053116.
- [28] G. Liu, G. Li, X. Qiu, L. Li, Synthesis of ZnO/titanate nanocomposites with highly photocatalytic activity under visible light irradiation, *J. Alloys Comp.* 481 (2009) 492–497.
- [29] P. Kundu, P.A. Deshpande, G. Madras, N. Ravishankar, Nanoscale ZnO/CdS heterostructures with engineered interfaces for high photocatalytic activity under solar radiation, *J. Mater. Chem.* 21 (2011) 4209–4216.
- [30] Y. Luo, Hydrothermal synthesis of one-dimensional ZnO/CdS core/shell nanocomposites, *Colloid J.* 71 (3) (2009) 370–374.
- [31] Y. Tak, S.J. Hong, J.S. Lee, K. Yong, Solution-based synthesis of a CdS nanoparticle/ZnO nanowire heterostructure array, *Cryst. Growth Des.* 19 (2009) 2627–2632.
- [32] R.G. Chaudhuri, S. Paria, Core/shell nanoparticles: classes, properties, synthesis mechanisms, characterization and applications, *Chem. Rev.* 112 (2012) 2373–2433.
- [33] D. Jiang, L. Cao, W. Liu, G. Su, H. Qu, Y. Sun, B. Dong, Synthesis and luminescence properties of core/shell ZnS:Mn/ZnO nanoparticles, *Nanoscale Res. Lett.* 4 (2009) 78–83.
- [34] P. Sudhagar, S. Chandramohan, R.S. Kumar, R. Sathyamoorthy, C.H. Hong, Y.S. Kang, Fabrication and charge-transfer characteristics of CdS QDs sensitized vertically grown flower-like ZnO solar cells with CdSe cosensitizers, *Phys. Status Solidi A* 208 (2) (2011) 474–479.
- [35] J. Chrysochoos, Recombination luminescence quenching of nonstoichiometric cadmium sulfide clusters by ZnTPP, *J. Phys. Chem.* 96 (7) (1992) 2868–2873.
- [36] A. Blanco, C. Lopez, R. Mayoral, H. Miguez, F. Meseguer, CdS photoluminescence inhibition by a photonic structure, *Appl. Phys. Lett.* 73 (1998) 1781–1783.
- [37] M. Qamar, S.J. Kim, A.K. Ganguli, TiO₂-based nanotubes modified with nickel: synthesis, properties and improved photocatalytic activity, *Nanotechnology* 20 (2009) 455703–455710.
- [38] J.M. Wu, T.W. Zhang, Photodegradation of rhodamine B in water assisted by titania films prepared through a novel procedure, *J. Photochem. Photobiol. A: Chem.* 162 (2004) 171–177.
- [39] P. Wilhelm, D. Stephan, Photodegradation of rhodamine B in aqueous solution via SiO₂@TiO₂ nano-spheres, *J. Photochem. Photobiol. A: Chem.* 185 (2007) 19–25.
- [40] J. Nayak, S.N. Sahu, J. Kasuya, S. Nozaki, CdS–ZnO composite nanorods: synthesis, characterization and application for photocatalytic degradation of 3,4-dihydroxy benzoic acid, *Appl. Surf. Sci.* 254 (2008) 7215–7218.
- [41] S. Wei, Z. Shao, X. Lu, Y. Liu, L. Cao, Y. He, Photocatalytic degradation of methyl orange over ITO/CdS/ZnO interface composite films, *J. Environ. Sci.* 21 (7) (2009) 991–996.
- [42] M.W. Xiao, L.S. Wang, Y.D. Wu, X.J. Huang, Z. Dang, Preparation and characterization of CdS nanoparticles decorated into titanate nanotubes and their photocatalytic properties, *Nanotechnology* 19 (2008) 015706–015713.
- [43] P. Qu, J. Zhao, T. Shen, H. Hidaka, TiO₂ assisted photodegradation of dyes: a study of two competitive processes in the degradation of RB in an aqueous TiO₂ colloidal solution, *J. Mol. Catal. A: Chem.* 129 (1998) 257–268.
- [44] G. Schmid, Nanoparticles, Wiley-VCH, Weinheim, 2004.